

AIR FLOW ANALYSIS AROUND THE AUTOGYRO FUSELAGE

Zbigniew Czyż¹, Ibrahim Ilhan², Mert Akcay³, Jacek Czarnigowski⁴

¹ Department of Thermodynamics, Fluid Mechanics and Aviation Propulsion Systems, Lublin University of Technology, 36 Nadbystrzycka Str., 20-618 Lublin, Poland, orcid.org/0000-0003-2281-1149, e-mail: z.czyz@pollub.pl

² Faculty of Engineering, Necmettin Erbakan University, Mehmet Hulusi Baybal, PhD. Cd. No:12, 42060 Konya, Turkey, e-mail: ibboilhan95@gmail.com

³ Department of Automotive Engineering, Cumhuriyet University, Kayseri Cd. 58070 Sivas/Merkez Turkey, e-mail: akcay.mert@outlook.com

⁴ Department of Thermodynamics, Fluid Mechanics and Aviation Propulsion Systems, Lublin University of Technology, 36 Nadbystrzycka Str., 20-618 Lublin, Poland, e-mail: j.czarnigowski@pollub.pl

Submitted: 2017-06-11 / Accepted: 2017-06-22 / Published: 2017-06-30

ABSTRACT

The paper presents the results of the simulation of the air flow around the gyroplane without the influence of the rotor and pusher propellers. Three-dimensional calculations were performed using ANSYS Fluent software. Based on the calculations, the values of the drag force and the lift force on each component of the rotorcraft were determined. Based on the results obtained, the effect of angle of attack on the aerodynamic forces was obtained.

KEYWORDS: CFD, Computational Fluid Dynamics, gyroplane, aerodynamics, lift force, drag force

ANALIZA PRZEPŁYWU POWIETRZA WOKÓŁ KADŁUBA WIATRAKOWCA

STRESZCZENIE

W pracy przedstawiono wyniki symulacji opływu modelu wiatrakowca bez wpływu wirnika nośnego oraz śmigła pchającego. Trójwymiarowe obliczenia wykonano za pomocą programu ANSYS Fluent. Na podstawie przeprowadzonych obliczeń wyznaczono wartości siły oporu oraz siły nośnej działające na poszczególne części składowe statku powietrznego. W oparciu o uzyskane wyniki otrzymano wpływ kąta natarcia na siły aerodynamiczne.

SŁOWA KLUCZOWE: CFD, obliczeniowa mechanika płynów, wiatrakowiec, aerodynamika, siła nośna, siła oporu

1. Introduction

Numerical investigations in comparison to the experimental research permit to validate assumptions at the design on early stage of the project and avoid costly process related to preparation of model or prototype to test bench. Using the CFD method, aerodynamic characteristics can be compiled and the aircraft's stability assessed. Simulation testing is a common tool in aircraft design. They allow, among other things, to determine their aerodynamic properties by establishing the external forces acting on them. Typically, these methods are less expensive and often make it possible to obtain data that are difficult to obtain in experimental research [1], [2]. Calculations of the aerodynamic properties of helicopter or gyroplane geometry have recently been the subject of numerous research papers. In work [3] the aerodynamic characteristics of the forces and moments acting on the helicopter fuselage are determined in two configurations: at the rotor blast in flight

conditions, as well as at a progressive speed. In work [4] simulation studies on flow around the helicopter have been carried out on various equipment configurations (camera, wings, pylons, reinforcement). These studies concerned the impact of individual helicopter units on aerodynamic characteristics. The impact of additional external components on the aerodynamic properties of the aircraft has been demonstrated. In many works (e.g. [3], [4], [5]) an additional VBM module was also used to simulate rotor operation. This module is based on the blade element theory, which defines the forces and moments acting on the elementary blade of width dR . Its operation is based on determining the increment of momentum generated by the rotor components.

2. Methodology and boundary conditions

The 3D model of the research object was done in CATIA v5 software. Figures 1 and 2 show a view of the geometric model of the gyroplane. The computational domain for the research object with the length of 0.632 m was made using an enclosure tool with a set distance for each direction equal 2 m to achieve total dimensions of 4,632 m x 4,294 m.

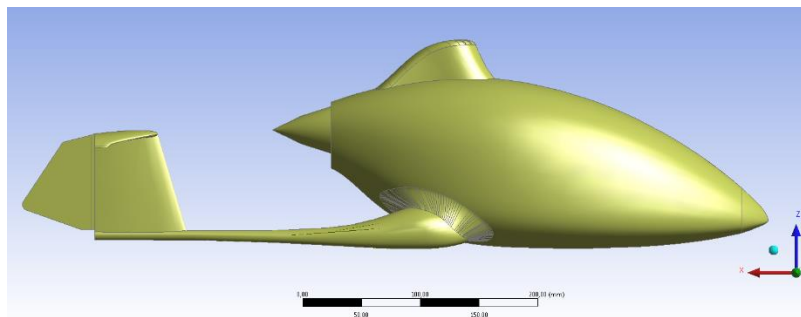


Fig. 1. Side view of the geometrical model of autogyro

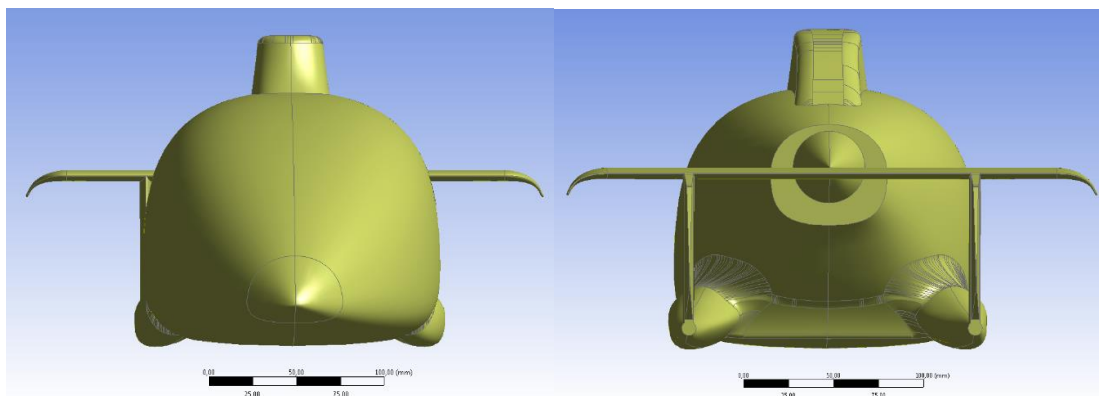


Fig. 2. Front view (left side) and back view (right side) of the geometrical model of autogyro

Numerical investigations were carried out using ANSYS / Fluent computational solver. The turbulence model $k-\omega$ SST was assumed for calculations. This was a model that combined two other models. The basic, most commonly used $k-\epsilon$ model did not work properly when modeling the boundary flow and did not reflect the phenomena occurring in the boundary layer. The results obtained with this model are reliable when there is a slow flow in which there is a turbulent area away from the boundary layer. A model that can be replaced with $k-\epsilon$ and which yields satisfactory results at flow close to the test wall is $k-\omega$ Wilcox. By combining these two models, one - $k-\omega$ SST was created, which used the Wilcox $k-\omega$ model at the boundary layer, and in the areas away from the research object wall $k-\epsilon$, so that the numerical results obtained were more reliable and comparable to the real ones. Therefore, for our consideration of the gyroplane fuselage in scale 1: 8 the $k-\omega$ SST model was chosen [1], [6].

Geometries similar to the considered case are most often discretized using tetrahedral elements. The size of the elements, their quantity and quality had a significant influence on the results of the calculations [7], [8]. Figure 3 shows the discrete model of the gyroplane tested. This is a tetrahedrons grid using the patch conforming algorithm. On the surface of the fuselage, a inflation with the option of smooth transition is defined.

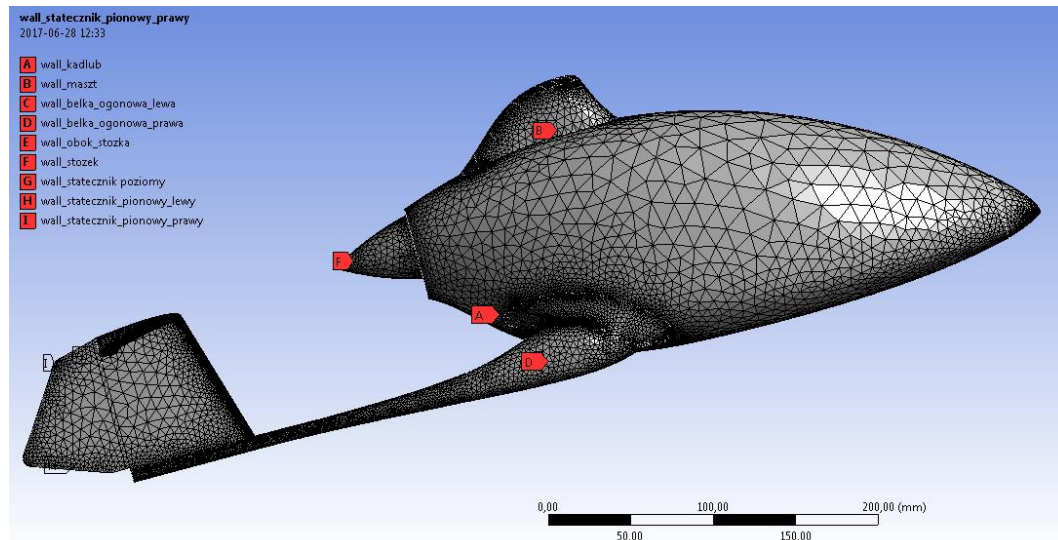


Fig. 3. General view of the gyroplane surface after discretization

The angle of attack of the fuselage α was calculated with a positive sign clockwise and the angle of the horizontal stabilizer adjustment was measured with respect to the plane XOY (positive up). On the front surface the velocity inlet boundary condition was given, and the pressure outlet boundary condition on the surface of the back wall [7]. For calculations, a steady state and pressure based simulation was selected. As a material, which flows around the research object being selected air and it assumes that the flow is incompressible and in defining the function of the material was selected: ideal - gas. Table 1 contains general settings of the numerical analysis. The turbulent intensity factor was set at 1%, while the turbulent length scale was defined as 0.3 m. Turbulence length scale l is the physical quantity associated with the size of the swirls that capture energy in turbulent motion [9]. Fully developed flows are limited by the dimensions of the duct. Approximately, the relation between the factor l and the physical dimension of the duct L is described by the relation $l = 0.07 L$.

Table 1. General settings of the numerical analysis

Basic settings	Type of calculation	Pressure-based		
	Time	Steady		
Turbulence model		k-omega (2-eqn) SST		
Materials	Gas	Air		
	Density	ideal-gas		
	Viscosity	Constant		
Boundary conditions	Inlet	Velocity	20 [m/s]	
		Turbulent intensity [%]	1	
		Turbulent Length Scale [m]	0.3	
	Outlet	Pressure- outlet	Gauge pressure 0 Pa	
		Turbulent intensity [%]	1	
Turbulent Length Scale [m]		0.3		

3. Results

Aerodynamic forces calculations were made for angles of attack from 0 ° to 20 °. Figures 4 to 8 illustrate the results of the pressure distribution on the surface of the aircraft concerned and the pressure and velocity contours on the symmetrical plane of the computational domain.

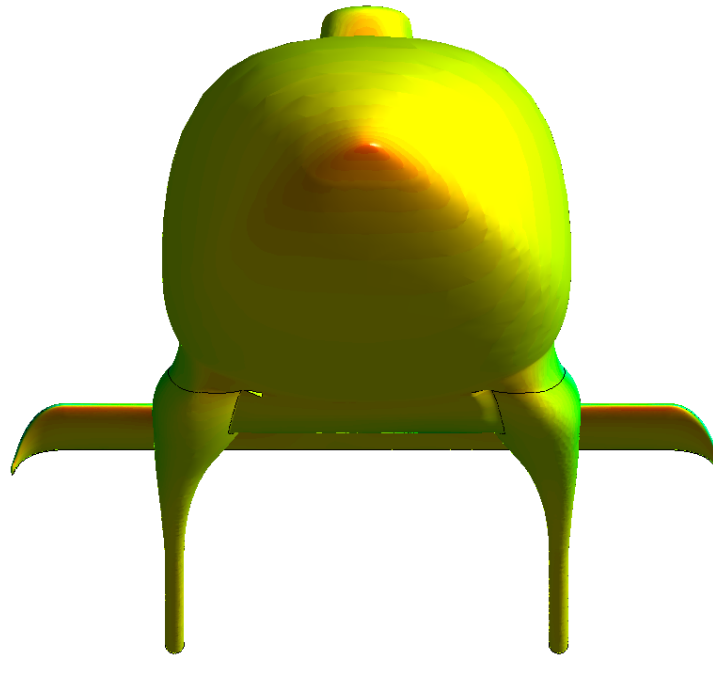
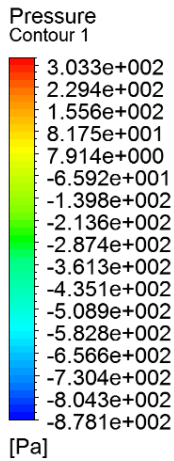


Fig. 4. Front view of the pressure contour on the autogyro surface

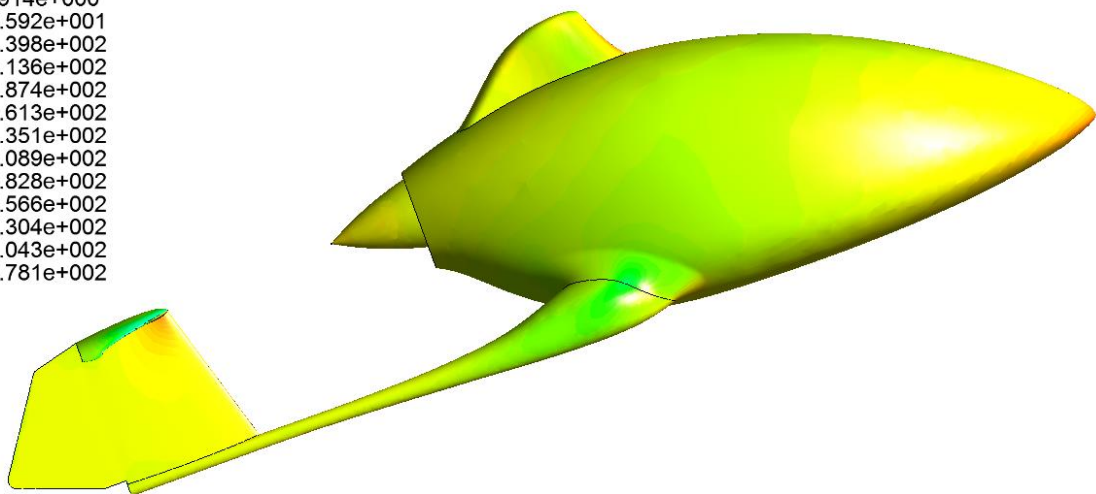
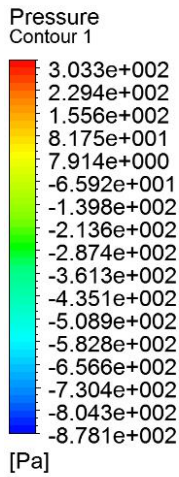


Fig. 5. Side view of the pressure contour on the autogyro surface

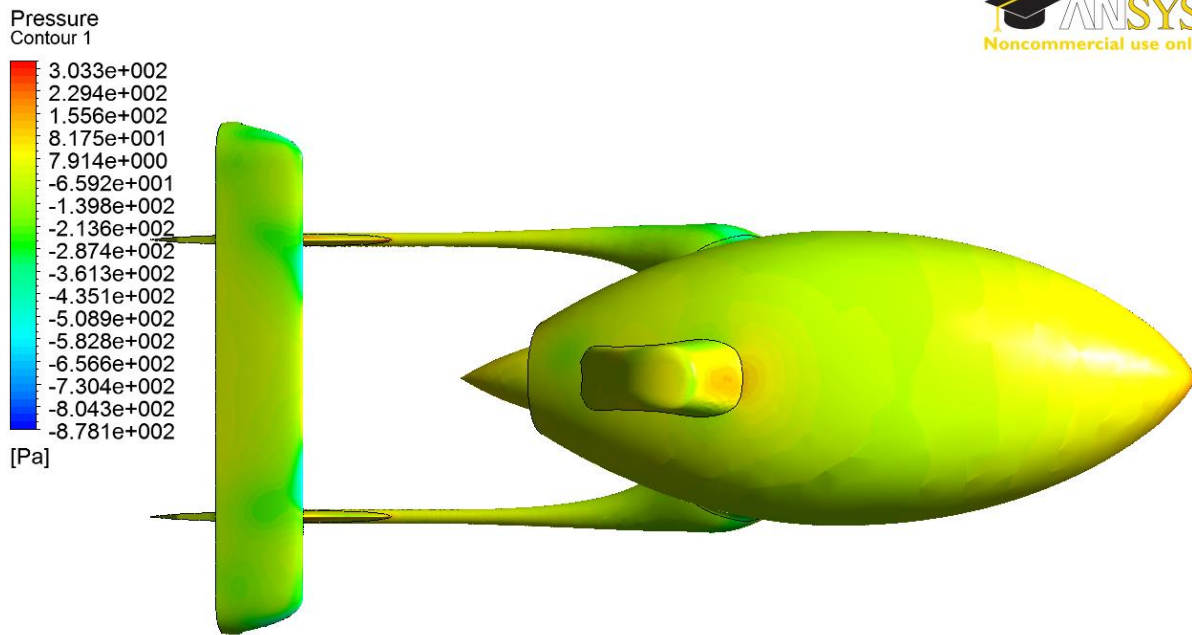


Fig. 6. Top view of the pressure contour on the autogyro surface

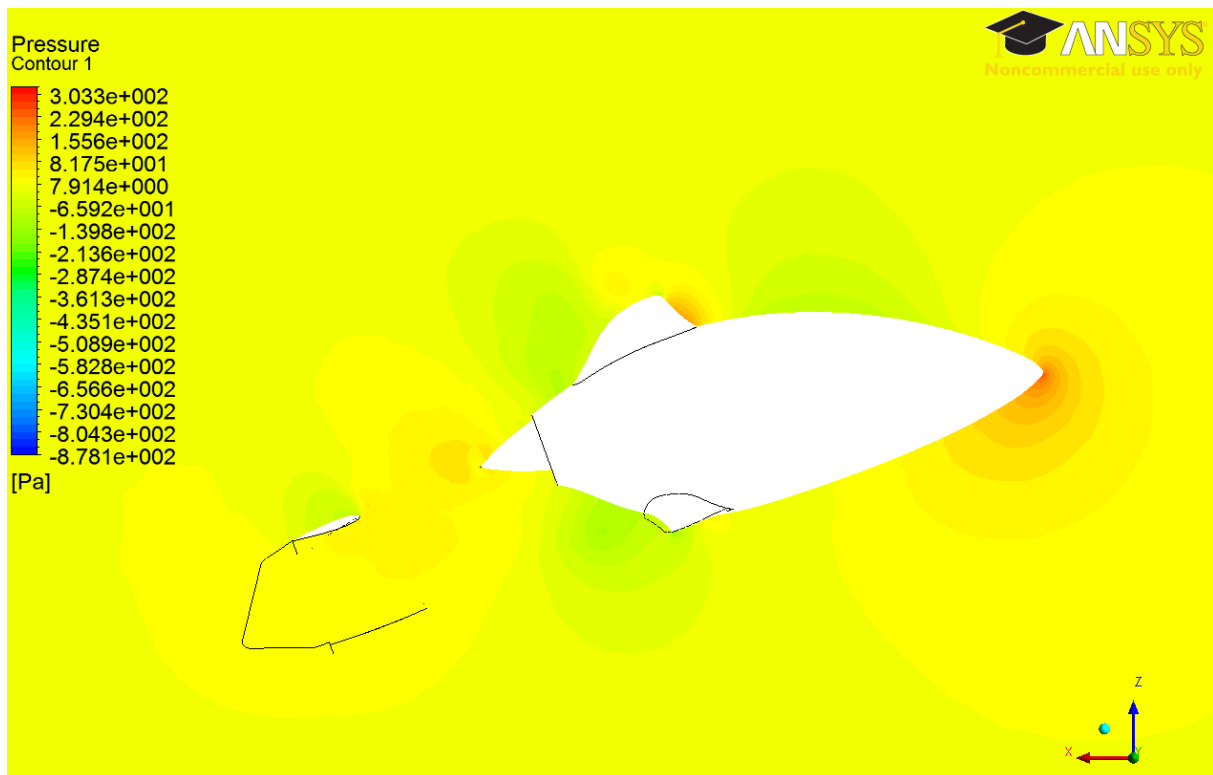


Fig. 7. Pressure contour on the symmetrical plane of the computational domain

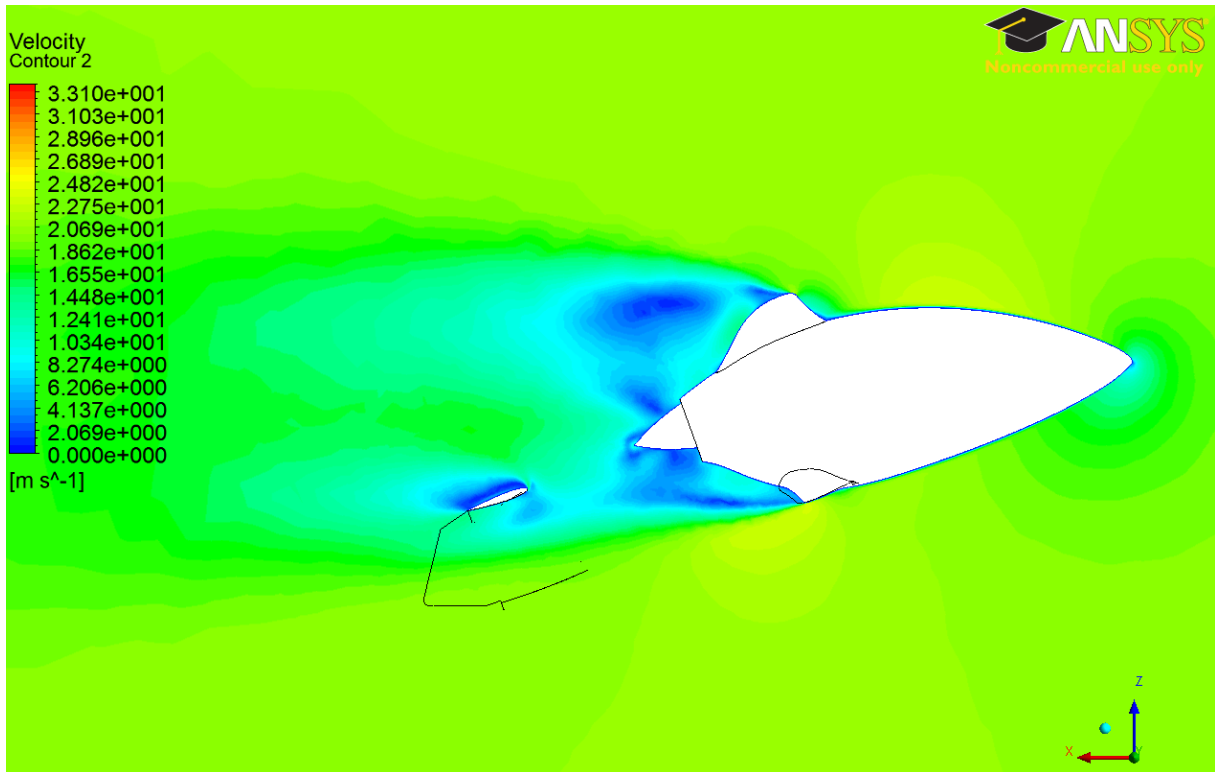


Fig. 8. Velocity contour on the symmetrical plane of the computational domain

Figure 9 shows the impact of angle of attack on the aerodynamic forces in the range of 0° to 20°.

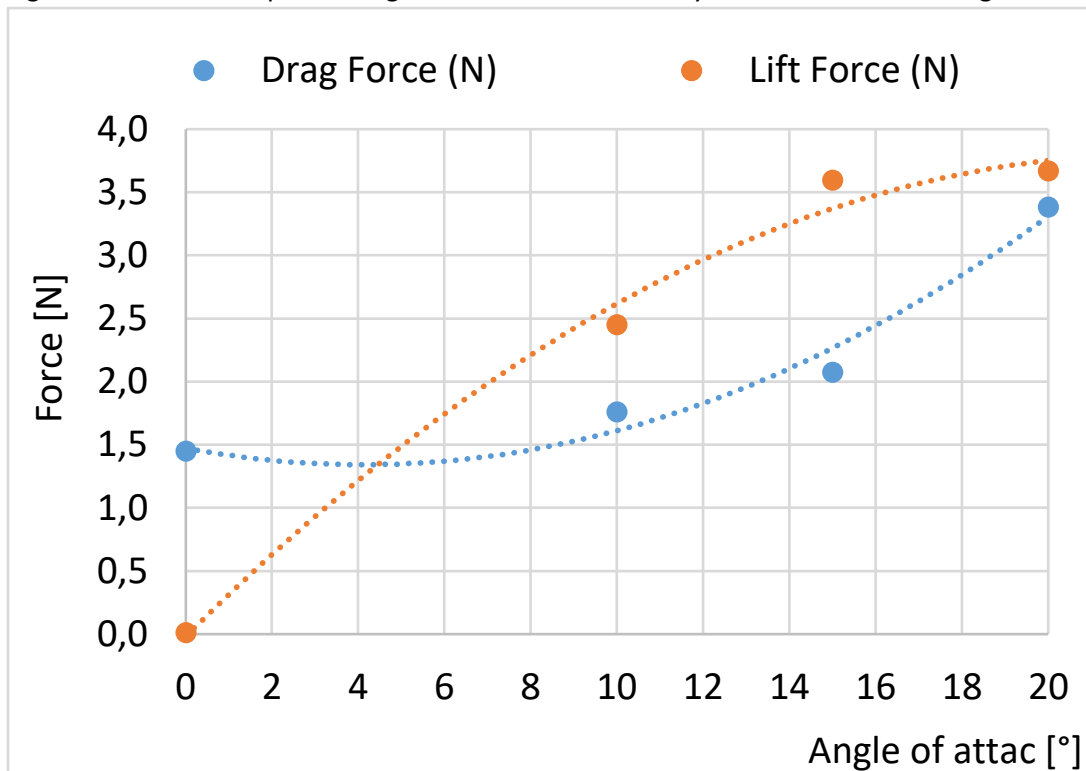


Fig. 9. Values of the lift force and drag force as a function of angle of attack

Table 2 shows the results of the calculation of aerodynamic forces broken divided into the individual components of the gyroplane tested for the selected angle. Results for other angles will be presented as bar graphs in Figures 10 and 11.

Table 2. Values of drag force and lift force for angle of attack 20°

No.	Name	Drag Force [N]	Lift Force [N]
1.	Tail beam - left	0.13883	0.08418
2.	Tail beam - right	0.12708	0.08829
3.	Fuselage	1.91952	2.08418
4.	Mast	0.13673	0.06112
5.	Back of the fuselage	0.01119	-0.00429
6.	Vertical stabilizer - left	0.07627	-0.01356
7.	Vertical stabilizer - right	0.07102	-0.01179
8.	Horizontal stabilizer	0.92155	2.52674
9.	Cone	-0.02007	0.01957
Total		3.38211	3.57907

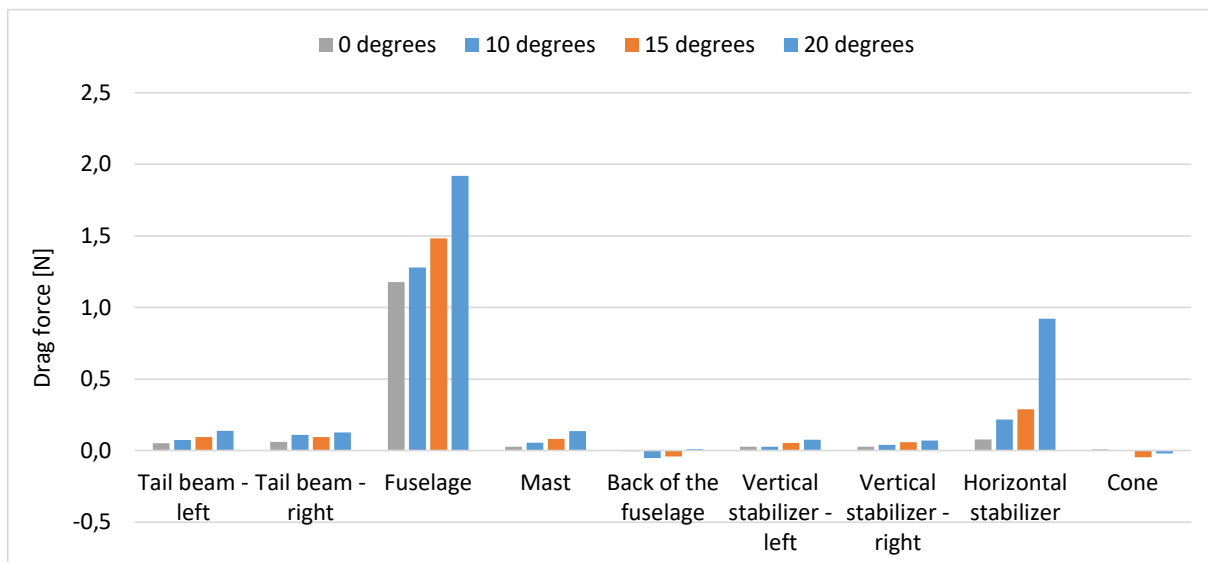


Fig. 10. Influence of angle of attack on the drag force generated by individual components of the gyrocopter

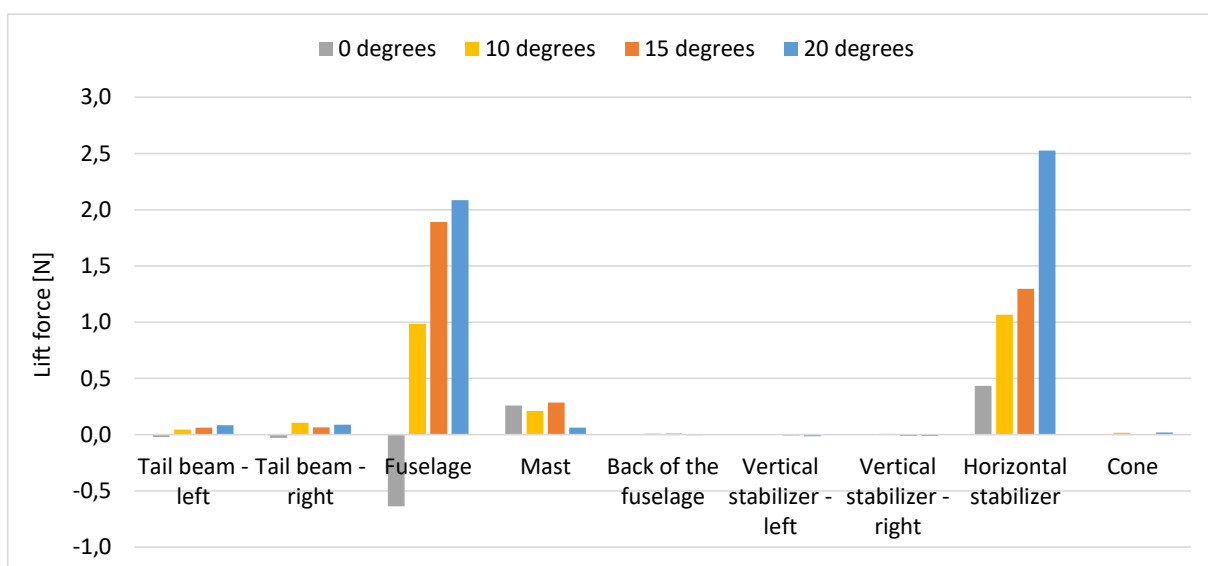


Fig. 11. Influence of angle of attack on the lift force generated by individual components of the gyrocopter

4. Conclusion

The paper presented the results of the simulation of the flow around the gyroplane without the influence of the rotor and pusher propellers. The calculations allowed to determine the values of the drag force and lift force acting on the individual components of the rotorcraft. Based on the results, the influence of the angle of attack on the aerodynamic forces and the percentage of forces generated by the individual components of the rotorcraft on the total value was obtained. For a steady flow rate of 20 m/s the maximum value of the velocity near the fuselage reached 33.1 m/s. The maximum overpressure on the fuselage surface was 303.3 Pa, while the negative pressure was -878.1 Pa. For the angle of attack 0° the maximum drag force generated the fuselage while the drag force generated by the horizontal stabilizer was 6.6% relative to the fuselage. Due to the zero angle of attack, the force generated by the fuselage was negative. In the case of the mast and the horizontal stabilizer, we can observe respectively 40.3% and 68% of the force relative to the fuselage. The horizontal stabilizer drag force increased as a function of angle of attack. For an angle of attack of 0° , the drag force was 0.07757 N, while for an angle of attack 20° it is 0.92155 N. As a result, the percentage of force generated by the horizontal stabilizer increased from 6.6% to 48%. In the case of lift force on the horizontal stabilizer at 20° it raised to 2.526 N, which was 21% higher than the fuselage. As shown in Figure 11, the horizontal stabilizer generated the largest force. This is related to the need to guarantee stability in this direction.

5. References

- [1] K. K. Versteeg, W. Malalasekera, *An introduction to Computational Fluid Dynamics*, Person Education Limited, London 2007.
- [2] A. Dziubiński, K. Grzegorzczak, J. Żółtak, "CFD analysis of external armour Influence on a helicopter aerodynamic Characteristics", *Transactions of the Institute of Aviation*, no. 218, pp. 20-27, 2011.
- [3] K. Grzegorzczak, "Analiza aerodynamiczna własności śmigłowca z uwzględnieniem nadmuchu wirnika nośnego", *Prace instytutu lotnictwa* no. 219, pp. 176-181, 2011.
- [4] A. Dziubiński, K. Grzegorzczak, "Study of the influence of helicopter's external components on the aerodynamic characteristics", *Transactions of The Institute of Aviation*, no. 218, pp. 11-19, 2011.
- [5] Z. Czyż, T. Łusiak, P. Magryta, "Badania numeryczne CFD wpływu usterzenia na charakterystyki aerodynamiczne", *Transactions of The Institute of Aviation - Prace Instytutu Lotnictwa*, no. 232, pp. 3-14, 2015.
- [6] D. C. Wilox, *Turbulence Modeling for CFD – Third Edition*. DCW Industries, 2006.
- [7] A. Lebediew, I. Strażewa, G. Sacharow, *Aeromechanika samolotu*, Wydawnictwo ministerstwa obrony Narodowej, 1958.
- [8] A. Dziubiński, *Generacja siatek obliczeniowych w symulacjach CFD. międzyuczelniane Warsztaty Inżynierskie*, 2010.
- [9] FLuent 13. *User's Guide*. Fluent Inc.